PHYSICAL REVIEW E **92**, 010901(R) (2015)

Asymptotic wave propagation in excitable media

Olivier Bernus
L'Institut de Rythmologie et Modélisation Cardiaque LIRYC, and Centre de Recherche Cardio-Thoracique, Inserm U1045, Université de Bordeaux, Bordeaux, France

Edward Vigmond
L'Institut de Rythmologie et Modélisation Cardiaque LIRYC, and Institut de Mathematique de Bordeaux, Université de Bordeaux, Bordeaux, France

(Received 5 February 2014; revised manuscript received 9 February 2015; published 8 July 2015)

Wave shape and velocity are important issues in reaction-diffusion systems, and are often the result of competition in media with heterogeneous conduction properties. Asymptotic wave front propagation at maximal conduction velocity has been previously reported in the context of anisotropic cardiac tissue, but it is unknown whether this is a universal property of excitable tissues where conduction velocity can be locally modulated by mechanisms other than anisotropy. Here, we investigate the impact of conduction heterogeneities and boundary effects on wave propagation in excitable media. Following a theoretical analysis, we find that wave-front cusps occur where local velocity is reduced and that asymptotic wave fronts propagate at the maximal translational conduction velocity. Simulations performed in different reaction-diffusion systems, including cardiac tissue, confirm our theoretical findings. We conclude that this property can be found in a wide range of reaction-diffusion systems with excitable dynamics and that asymptotic wave-front shapes can be predicted.

DOI: 10.1103/PhysRevE.92.010901 PACS number(s): 05.45.−a, 87.19.Hh, 87.10.−e

I. INTRODUCTION

Nonlinear waves of excitation govern a wide range of phenomena, typically described by reaction-diffusion equations, and including, for example, flame-front propagation [1], Belousov-Zhabotinsky chemical reactions [2], morphogenesis of amoeba [3], intracellular calcium waves [4], and electrical signaling in neural [5] and cardiac tissues [6]. The asymptotic wave-front shape and velocity are important properties of wave propagation and pattern formation in such media that have not yet been properly addressed in systems with spatially varying conduction properties.

Wave competition has previously been observed in the heterogeneous Belousov-Zhabotinsky reaction [7] showing a gradual invasion of the slower portions of the wave front by the faster leading peaks. This results in a stationary wave front whose shape and velocity are primarily determined by the propagation dynamics of the faster portion [8]. A similar behavior was found more recently in models of homogeneous but anisotropic cardiac tissue. In this case, heterogeneity in conduction properties is obtained through spatially varying myofiber orientation [9]. Computational studies showed that anisotropy could give rise to trailing intramural cusps in layers where propagation is locally perpendicular to the fiber orientation [10]. These cusps in the wave front can move across layers and disappear at tissue surfaces where they cause sudden apparent wave-front accelerations. Subsequent propagation is asymptotic and can be described by translational wave motion at the maximal longitudinal conduction velocity, irrespective of local fiber orientation [11]. These findings were verified theoretically and numerically in Ref. [11] and indirectly through surface conduction velocity measurements in intact heart optical mapping experiments [12]. More recently, a geometric theory based on non-Euclidean metrics was proposed to explain this observation in anisotropic heart models [13]. However, it remains unknown whether these observations on asymptotic wave propagation are general features of excitable media with heterogeneous conduction properties, especially those which affect active behavior.

In the present Rapid Communication, we show that the occurrence of cusp waves and asymptotic wave propagation at the fastest conduction velocity are universal properties of wave propagation in excitable media, irrespective of the mechanism leading to local dispersion of conduction velocities. We primarily demonstrate these phenomena in cardiac tissue with heterogeneous conduction properties across the thickness of the ventricular wall, but demonstrate that our analysis holds for any type of reaction-diffusion system.

II. THEORETICAL ANALYSIS OF ASYMPTOTIC PROPAGATION AND CUSP WAVES

Let us first consider the asymptotic wave-front propagation. We follow the approach described in Ref. [11] to derive analytically the wave-front shape and its translational velocity. We start with the case of an isotropic slab of thickness L with a plane wave originating at $x = 0$ and propagating in the positive x direction. The z direction denotes the transmural direction across the thickness of the slab. For ease of mathematical derivation, consider transmural heterogeneous tissue properties leading to heterogeneities in conduction velocity $c(z)$ (other types of heterogeneities can be treated in a similar manner). The wave-front position in the x direction is denoted by F. The initially plane wave front will be deformed by the transmural conduction heterogeneity and therefore F will show z dependence. Assuming a constant asymptotic translational velocity c_x exists, we find that the asymptotic wave front shape is given by the equation

$$\frac{dF}{dz}(z) = \pm\sqrt{\left(\frac{c_x}{c(z)}\right)^2 - 1}, \tag{1}$$

or

$$F(z) = \pm \int_0^z \sqrt{\left(\frac{c_x}{c(z)}\right)^2 - 1}\, dz + F_0, \qquad (2)$$

with $F_0 = F(0)$ an integration constant and where the sign determines the slope of the wave front.

Consider a wave front with a single leading peak forming in the layer $z_{\max}$ where the medium properties yield maximal conduction velocity $c_{\max}$. Since the leading peak is an extremum of $F(z)$, we readily find from Eq. (1) that $c_x = c_{\max}$. Remarkably, and similar to the case of anisotropy, we find that the translational velocity is entrained to the maximal conduction velocity in the heterogeneous reaction-diffusion system.

Consider now the case of a wave front with initially two leading peaks forming in two distinct layers z_1 and z_2 where the conduction velocity function has local maxima c_1 and c_2. Without any loss in generality we consider $z_1 < z_2$. A trailing cusp will be formed at a depth $z_1 < z_0 < z_2$ where the conduction velocity has a local minimum. The cusp effectively splits the wave front in two portions: the lower having a quasiasymptotic translational velocity c_1 and the upper c_2. If $c_1 > c_2$, the cusp will move towards and disappear at the $z = L$ medium boundary. Once the cusp has disappeared at the medium boundary, the problem is reduced to the previous case of an asymptotic wave front with a single leading peak and maximal translational velocity $c_x = c_1$. A similar reasoning applies to the case where $c_2 > c_1$. In the special case of two leading peaks with $c_1 = c_2$, a cusp will be observed in the layer with minimal conduction velocity between the two leading peaks. However, in this case, the cusp will not vanish at a medium boundary and will remain in the same layer once asymptotic propagation is reached.

III. COMPUTATIONAL EXAMPLES IN CARDIAC TISSUE

In order to verify our theoretical predictions, we ran simulations in a widely studied excitable medium, i.e., cardiac tissue. We ran monodomain simulations on a two-dimensional (2D) finite element grid measuring 8×0.8 cm discretized into quadrilaterals with edge lengths of 100 μm. The transmural direction was defined from epicardium ($z = 0$) to endocardium ($z = L$). The CARP cardiac simulator [14] solved the system with an explicit method and a time step of 20 μs. Propagation was initiated on the entire left edge of the tissue by applying a 1 ms long transmembrane current pulse. To describe electrophysiological behavior of nonischemic tissue, the Luo-Rudy ionic model was used [15], while for ischemic tissue, the Mahajan rabbit ionic model was implemented [16]. For ischemic tissue sodium and calcium conductance was set to 75%, the extracellular potassium concentration was elevated to 12 mM, intracellular potassium concentration was lowered to 152.5 mM, and an adenosine triphosphate (ATP)-sensitive potassium channel was introduced with an adenosine diphosphate (ADP)/ATP ratio of 0.0063. Tissue conductivity was set to 0.174 S/m in all cases. Conduction velocity was measured as the inverse gradient of the activation time map. Translational conduction velocity was obtained by projecting the conduction velocity onto the x axis.

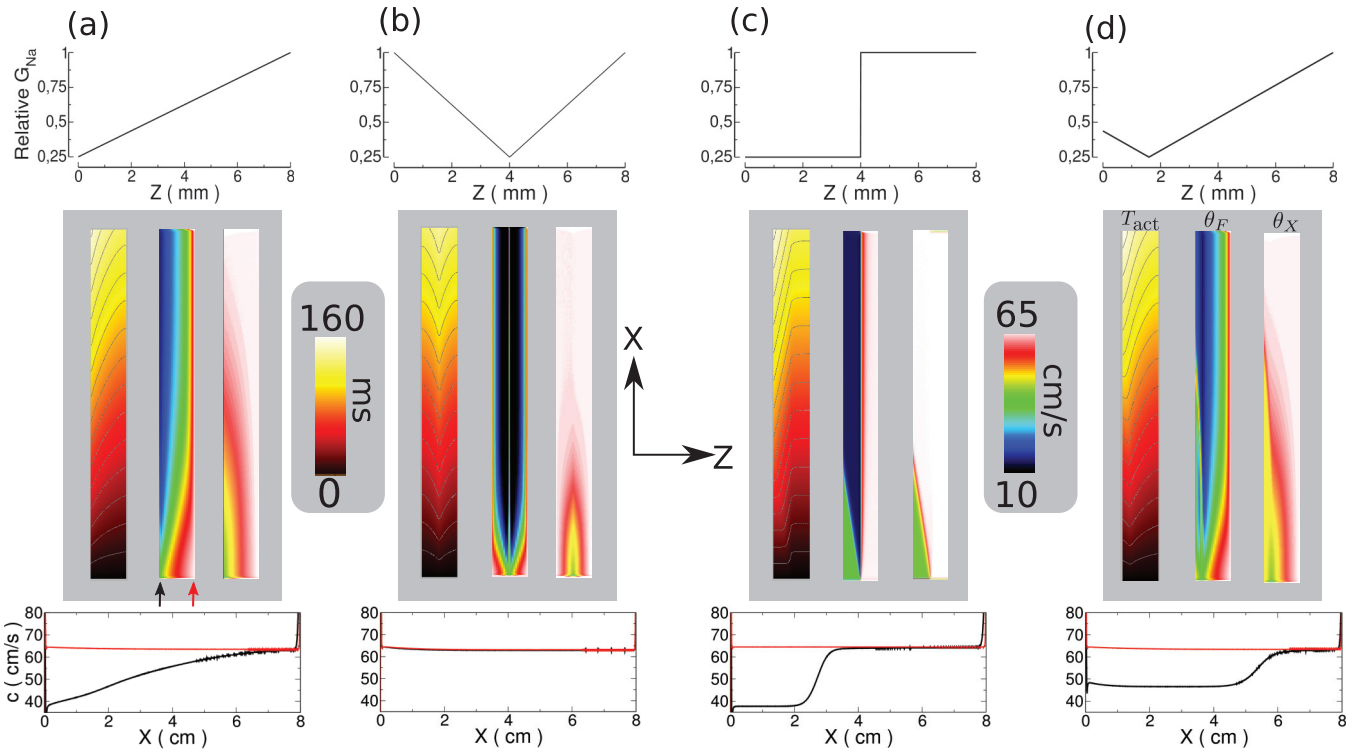

FIG. 1. (Color) Asymptotic wave propagation in a slab of cardiac tissue with four different transmural g_{Na} profile (top panels). The middle panels represent T_{act}, c, and c_x, respectively (black and red arrows indicate the epicardial and endocardial surfaces, respectively), while the bottom panel show the measured conduction velocity on epicardium (black) and endocardium (red).

A. Transmural ion channel heterogeneity

In a first set of simulations, we varied the transmural conduction velocity by implementing various gradients of the sodium channel conductance g_{Na}. Figure 1 shows the resulting intramural propagation dynamics for four different scenarios: (a) a linear transmural g_{Na} gradient with minimum at the epicardium ($z = 0$ mm) and maximum at endocardium ($z = 8$ mm), (b) a piecewise-linear transmural g_{Na} gradient with a minimum in the middle of the slab ($z = 4$ mm) and equal conductances at the epicardium and endocardium, (c) a transmural step function with low g_{Na} on the epicardial side and high g_{Na} on the endocardial side of the slab, and (d) a piecewise-linear transmural g_{Na} gradient with a minimum at $z = 1.8$ mm and largest conductance at the endocardium. The upper panels in Fig. 1 illustrate these four different transmural g_{Na} profiles. The middle panels show for each case the transmural activation time (T_{act}) map, the wave-front conduction velocity c map, and the translational velocity c_x map following plane stimulation at $x = 0$. The lower panels show conduction velocities measured on the epicardium (black) and endocardium (red) as a function of distance from stimulus (x).

In the case of a linear transmural gradient [Fig. 1(a)] we observe the formation of a wave front with a leading peak at the endocardium, where g_{Na} is maximal. The wave reaches the asymptotic regime with no further changes in wave-front shape or conduction velocity at about $x = 6$ cm, as can be inferred from the T_{act} and c maps. At this point, the translational velocity c_x is maximal at all depths throughout the slab. A constant and maximal conduction velocity is observed on the endocardium, but a gradually increasing velocity is observed on the epicardium until it reaches the maximal conduction velocity. Hence, even though the epicardial g_{Na} is reduced, the maximal conduction velocity will be reached at some distance away from the pacing site on this surface.

In the second case [Fig. 1(b)], a wave front with two leading peaks at the epicardium and endocardium, respectively, is formed with an initially trailing cusp at the middle of the slab. The asymptotic regime is rapidly reached, at which point the translational velocity is maximal at all depths. The conduction velocities measured at the tissue surfaces remain constant and maximal, consistent with maximal g_{Na} at both surfaces. Note that the effect of wave-front curvature on propagation velocity is apparent at the cusp where c shows a local maximum.

In the third case [Fig. 1(c)], the endocardial portion ($4 < z \leqslant 8$ mm) propagates faster than the epicardial portion of the wave front ($0 \leqslant z < 4$ mm). This leads to an initially transmural steplike wave front. As the wave propagates further into the tissue, the wave-front orientation in the epicardial portion changes gradually. The wave reaches its asymptotic regime within a few cm from the pacing site, at which point the wave-front orientation has acquired a constant acute angle with respect to the epicardium in the lower portion of the slab. The conduction velocity measured on the epicardium also shows a sudden increase at this point and the wave propagates at maximal translational conduction velocity from this point onward.

Finally, in the fourth case [Fig. 1(d)], two leading peaks are also observed at the epicardium and endocardium, but now with the maximal velocity on the endocardium and an intramural cusp located closer to the epicardium. As the wave propagates, the faster portion of the wave front gradually overtakes the slower portion and the cusp moves towards the epicardial surface. The cusp eventually disappears at the epicardium, at which point the wave reaches its asymptotic regime at maximal translational velocity c_x at all depths. A sudden increase in epicardial conduction velocity is also observed in this case.

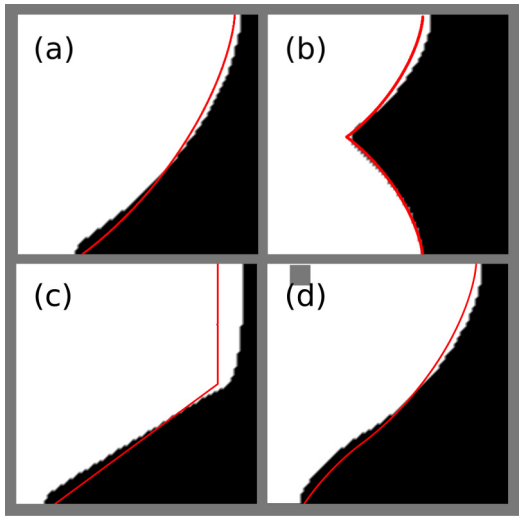

FIG. 2. (Color online) Comparison between the theoretically predicted (solid line) and simulated (white) asymptotic wave-front shape.

As can be inferred from Fig. 1, the distance at which the asymptotic regime and the maximal translational velocity are reached depends on the extent and type of heterogeneity.

We verified the validity of Eq. (2) by comparison with the simulated asymptotic wave shapes shown in Fig. 1. First, we determined computationally the dependence of c on g_{Na} and found the following relationship in the Luo-Rudy model, $c(g_{Na}) = 0.0307 + 0.378\sqrt{g_{Na}/23 - 0.21}$, where g_{Na} is expressed in $\mu A/cm^2$. Next, we numerically integrated Eq. (2) with $c[g_{Na}(z)]$ for the four different cases described above. Figure 2 shows the results where the thick solid line indicates the theoretically predicted wave front overlaid on the simulated asymptotic wave shapes from Fig. 1 (white on black background). We observe in all cases a good match between theory and simulation. This was further verified by quantifying the lateral extent of each asymptotic wave front (i.e., the difference in x coordinates between the leading and trailing edges) in each case: (a) 5.1 (theory) vs 5.4 (simulation) mm, (b) 2.5 vs 2.5 mm, (c) 5.4 vs 6.6 mm, and (d) 5.6 vs 6.1 mm. The relative difference between theory and simulation ranges from 0% to 18%.

B. Bath-loading effects on intramural propagation

The extracellular bath (such as blood *in vivo* or saline solution in experiments) provides a low resistance pathway for extracellular currents resulting in a faster wave propagation at the tissue surface [17]. Several simulation studies have shown that this bath-loading effect can result in significantly

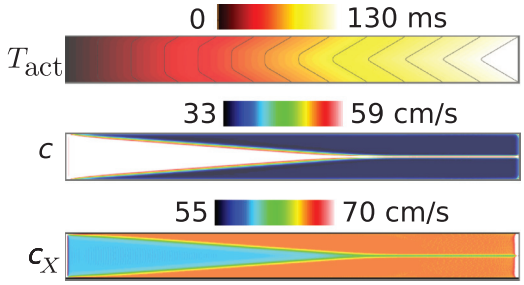

FIG. 3. (Color) Effect of bath loading on transmural activation patterns and conduction velocities.

curved intramural wave fronts, but without investigating its mechanisms. Here, we find that intramural wave-front dynamics in the presence of a tissue bath is a special case of our general description above with fast conducting layers at the epicardium and endocardium. Indeed, our theoretical analysis predicts that an initially plane wave front will gradually evolve towards its asymptotic shape with two leading peaks at the tissue boundaries, a cusp in the middle of the slab, and a translational velocity equal to the maximal conduction velocity. This prediction was verified numerically and the results are shown in Fig. 3.

C. Impact of regional ischemia on intramural propagation

Regional ischemia significantly increases electrophysiological and conduction heterogeneity [18]. Here, we investigated the effects of regional conduction velocity reduction due to tissue changes related to ischemia. Acute ischemia was simulated in the endocardial half of the tissue and a transmural plane wave was simulated as in previous cases (Fig. 4). In accordance with our theoretical predictions and similar to the case presented in Fig. 1(c), we observe a wave that rapidly reaches an asymptotic regime at which point the translational velocity is maximal throughout the tissue slab. Interestingly, the apparent conduction velocity measured at this point on the pathological (ischemic) endocardial surface is much higher than what would normally be expected in ischemic tissue [18].

IV. DISCUSSION AND CONCLUSION

To date, theoretical, numerical, and experimental studies of asymptotic wave propagation in cardiac tissue have primarily focused on the effects of structural heterogeneities and changing fiber orientation, or in mathematical terms, a spatially varying diffusion tensor [10–13]. These studies have shown that cusp waves can occur in regions where propagation is perpendicular to the local fiber orientation, i.e., locally the slowest, and more importantly that, at a distance from the pacing site, waves reach an asymptotic translational regime propagating at the maximal conduction velocity [10,11].

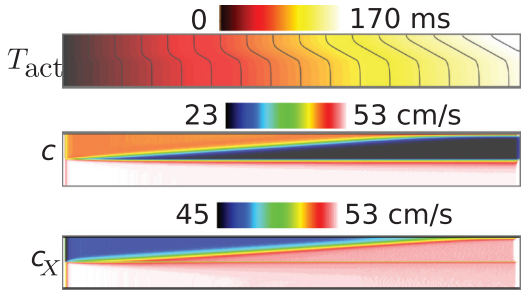

FIG. 4. (Color) Effect of subendocardial ischemia on transmural activation patterns and conduction velocities.

In the present study, we show that previous findings on asymptotic wave propagation invariably and universally hold in the presence of electrophysiological heterogeneities that lead to spatial dispersion of conduction velocity (i.e., spatially varying reaction parameters that impact on excitability). Specifically, we find that cusps can be formed in the wave front in regions where conduction velocity is depressed, that these cusps can move along the wave front, and that in all cases, waves reach an asymptotic translational regime propagating at the maximal local conduction velocity. Our results have important implications for the experimental measure of conduction velocity and its interpretation. Indeed, we find that if such measurement is performed at a distance from the wave origin, measured conduction velocity at the surface will always be maximal. Therefore, such measurement may not be representative of the local electrophysiological or structural properties, and the disease state (such as ischemia) of the tissue. Given that measurement of conduction velocity near the stimulation site is furthermore complicated by virtual electrode effects, extreme caution should be exerted when measuring and interpreting conduction velocities in the structurally and electrophysiologically heterogeneous heart.

Recent theoretical and numerical studies have shown that in homogeneous anisotropic media the description of wave propagation could be greatly simplified by considering the inverse diffusion tensor as a metric in a non-Euclidean space [19–21]. This approach allowed [13] to explain the earlier observation of asymptotic wave propagation at maximal conduction velocity within a geometrical framework where electrophysiological distances are defined with respect to the diffusion metric. Even though our study has focused on heterogeneities in the reaction term, the previous geometrical analysis and concept of electrophysiological distance introduced by Ref. [13] could still be applied in our case through the construction of an equivalent diffusion tensor in an homogeneous medium that would phenomenologically reproduce wave propagation of an heterogeneous medium. This can easily be achieved knowing that c should scale as $\sqrt{D}$, where D is the scalar diffusion coefficient in an isotropic medium. In this way, one can also show that the previously obtained result of asymptotic wave propagation at maximal speed should invariably hold for any type of heterogeneity.

Although we have focused on cardiac tissue to illustrate our findings, our theoretical analysis does not make any assumption on the choice of model or parameters. We therefore further verified our theoretical predictions in two other heterogeneous excitable media: the two-variable Oregonator model with a single diffusing variable for the Belousov-Zhabotinsky (BZ) reaction [22] and the FitzHugh-Nagumo (FHN) [23] models. Simulation results are presented in Fig. 5. In both cases we have investigated wave-front propagation in a two-dimensional medium perpendicular to a gradient in excitability properties.

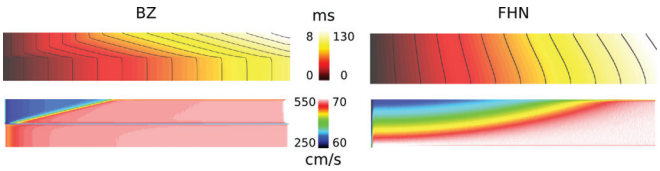

FIG. 5. (Color) Asymptotic wave propagation in the heterogeneous Oregonator (BZ) and the Fitzhugh-Nagumo equations (FHN). For the Oregonator, ϵ was varied in a stepwise manner with a value 0.5 in the bottom half of the medium and a value of 1.5 in the top. Activation is show with 0.5 ms isochrones in the upper panel, and c_x below. The FHN equations were implemented with a linear increase in the v_p parameter from 0.85 at the bottom to 1.05 at the top. Activation is shown with 10 ms isochrones (top panel) and c_x below. In both cases asymptotic wave propagation at the maximal translational conduction velocity can be observed.

In the Oregonator model we have simulated a stepwise gradient in the parameter ϵ, whereas in the FHN model we implemented a linear change in the parameter v_p. All other parameters remained unchanged from the original publications. In both cases, we find the expected asymptotic behavior with the translational conduction velocity reaching a steady state at the maximal conduction velocity. Our findings should thus hold for a wide class of reaction-diffusion systems.

ACKNOWLEDGMENT

This work was supported by a grant from the Agence Nationale de la Recherche through the program "Investissements d'Avenir" (ANR-10-IAHU04-LIRYC).

[1] G. I. Sivashinsky, Acta Astronaut. **4**, 1177 (1977).
[2] A. N. Zaikin and A. M. Zhabotinsky, Nature (London) **225**, 535 (1970).
[3] F. Siegert and C. J. Weijer, Proc. Natl. Acad. Sci. USA **89**, 6433 (1992).
[4] J. Lechleiter, S. Girard, E. Peraltal, and D. Clapham, Science **252**, 123 (1991).
[5] A. L. Hodgkin and A. F. Huxley, J. Physiol. **117**, 500 (1952).
[6] D. Noble, J. Physiol. **160**, 317 (1962).
[7] I. Sendiña-Nadal, M. Gómez-Gesteira, V. Pérez-Muñuzuri, V. Pérez-Villar, J. Armero, L. Ramírez-Piscina, J. Casademunt, F. Sagués, and J. M. Sancho, Phys. Rev. E **56**, 6298 (1997).
[8] J. Armero, A. M. Lacasta, L. Ramírez-Piscina, J. Casademunt, J. M. Sancho, and F. Sagués, Phys. Rev. E **56**, 5405 (1997).
[9] D. Streeter, in *Handbook of Physiology*, edited by E. Page, H. A. Fozzard, and R. J. Solaro (American Physiological Society, Bethesda, MD, 1979), Sec. 2, Vol. I, pp. 61–112.
[10] J. Keener and A. V. Panfilov, J. Cardiovasc. Electrophysiol. **4**, 412 (1993).
[11] O. Bernus, M. Wellner, and A. M. Pertsov, Phys. Rev. E **70**, 061913 (2004).
[12] C. W. Zemlin, O. Bernus, A. Matiukas, C. J. Hyatt, and A. M. Pertsov, Biophys. J. **95**, 942 (2008).
[13] R. J. Young and A. V. Panfilov, Proc. Nat. Acad. Sci. USA **107**, 15063 (2010).
[14] E. J. Vigmond, M. Hughes, G. Plank, and L. J. Leon, J. Electrocardiol. **36**, 69 (2003).
[15] C. H. Luo and Y. Rudy, Circ. Res. **68**, 1501 (1991).
[16] A. Mahajan *et al.*, Biophys. J. **94**, 392 (2008).
[17] M. J. Bishop, E. Vigmond, and G. Plank, Biophys. J. **101**, 2871 (2011).
[18] R. M. Shaw and Y. Rudy, Circ. Res. **80**, 124 (1997).
[19] M. Wellner, O. M. Berenfeld, J. Jalife, and A. M. Pertsov, Proc. Natl. Acad. Sci. USA **99**, 8015 (2002).
[20] H. Verschelde, H. Dierckx, and O. Bernus, Phys. Rev. Lett. **99**, 168104 (2007).
[21] H. Dierckx, O. Bernus, and H. Verschelde, Phys. Rev. Lett. **107**, 108101 (2011).
[22] J. J. Tyson and P. C. Fife, J. Chem. Phys. **73**, 2224 (1980).
[23] J. M. Rogers and A. D. McCulloch, J. Cardiovasc. Electrophysiol. **5**, 496 (1994).